Chemical effects in the manganese $3s \rightarrow 2p$ x-ray emission that follows resonant and nonresonant photon production of a $2p$ hole

J. Jiménez-Mier*
Instituto de Ciencias Nucleares, UNAM, 04510 México Distrito Federal, Mexico

D. L. Ederer and T. Schuler
Department of Physics, Tulane University, New Orleans, Louisiana 70118, USA
(Received 16 March 2004; published 30 July 2004)

Spectra for the manganese $3s \rightarrow 2p$ x-ray emission after resonant and nonresonant photon excitation of a $2p$ electron are presented for metallic manganese, MnF_2, MnO, and $LaMnO_3$. The absorption and emission spectra are compared with the results of free-ion calculations for Mn^{2+} and Mn^{3+}. The experimental absorption spectrum of MnF_2 is in very good agreement with the calculation for Mn^{2+}, while the absorption of the other compounds is found to be a superposition of Mn^{2+} and Mn^{3+}. There are noticeable differences among the compounds, both in the relative positions and intensities of the emission peaks. The resonant emission spectra from MnF_2 is dominated by decay from the $2p^5 3d^6$ resonant configuration, while "normal" fluorescence is found to predominate in $LaMnO_3$. In metallic manganese and MnO the emission spectra are well described as a superposition of these two extreme cases.

DOI: 10.1103/PhysRevB.70.035216 PACS number(s): 78.70.Ck, 78.70.En

I. INTRODUCTION

Transition-metal compounds have a wide range of interesting electronic and magnetic properties that have made them the subject of numerous studies. Located right in the middle of the $3d$ row, manganese forms compounds that can be used to study different aspects of transition-metal compounds ranging from the effect of intra-atomic electron-electron correlation to charge transfer. Knowledge of these properties is important for both a basic understanding of the electronic structure of these compounds and to understand their behavior in many applications.

Inner-shell spectroscopies are well-established tools for the study of the electronic structure and thus have been extensively applied to manganese compounds. X-ray absorption spectroscopy (XAS) across the L absorption edge in Mn has been used to determine, among other things, the manganese oxidation state in different compounds.[1–6] This is possible because in XAS one obtains information about the conduction band, of $3d$ character. In this regard the ligand-field multiplet theory[7] has proven to be an invaluable tool in the interpretation of the results. Complementary to XAS, x-ray emission spectroscopy (XES) provides information about the density of states of occupied levels that participate in the decay process after the production of an inner-shell hole. One can also study photoexcitation processes that involve the resonant promotion of an inner-shell electron into a discrete or quasidiscrete state, followed by the emission of a photon to fill the inner-shell hole. An analysis of the energy loss in this x-ray Raman-scattering process provides information about the energy levels of the ground state. In particular, the $2p \rightarrow 3d$ resonant excitation with the subsequent decay of the $2p$ hole by photon emission is particularly well suited to study the partially filled $3d$ shell in manganese compounds. Early studies of valence emission in MnO showed that useful quantitative information about low-energy d to d dipole-forbidden excitations could be obtained.[9] That work also showed that a free-ion calculation in a two-step picture,[9] was adequate for a direct comparison with experiment. Chemical effects in both x-ray absorption and resonant valence x-ray emission in several manganese complexes have been studied in detail.[2,3,5] Recently, attention has been given to the process in which the $2p$ core hole is filled by emission from the $3s$ shallow inner shell. In addition to the well-known advantages of the valence photon-in–photon-out processes,[10] detection of emission from the $3s$ core level is not affected by self-absorption,[11] and one is therefore allowed to directly compare emission from different samples. The $3s$-hole width is, however, rather large (of the order of a few eV), and this results in broad emission features. Also, the emission process is strongly affected by electron-electron correlation, especially by interaction between the configuration with a $3s$ hole in the final state with the configuration with two $3p$ holes,[12–14] something that reflects the fact that in these compounds intra-atomic many-body effects are as important as the interatomic many-body effects.[8] This correlation effect in the $3s \rightarrow 2p$ emission was studied[12] for one value of the excitation energy in $MnFe_2O_4$, and is the subject of independent work[14] for a whole range of excitation energies in MnF_2. In that article,[14] we showed that in this ionic compound, the observed resonant spectra can be interpreted in terms of a relatively simple Mn^{2+} free-ion calculation that includes the interaction between the $3d^5$ ground-state configuration and the configurations with a single hole in the $3s$ subshell ($3s3d^6$), and the configuration with two holes in the $3p$ subshell ($3p^4 3d^7$). We also proved that a comparison with a free-ion calculation also gives good results for nonresonant excitation, provided that only the states with a $2p$ hole coupled to the $3d^5\ ^6S$ high-spin outer shell are considered.

In this article we present a comparison of experimental results for resonant and nonresonant manganese $3s \rightarrow 2p$ emission in metallic manganese and in the compounds MnO and $LaMnO_3$. We use our previous results[14] for MnF_2 as a reference. Manganese is nominally Mn^{2+} in MnF_2 and MnO, while it appears as Mn^{3+} in $LaMnO_3$. Therefore, the Mn^{2+} free-ion calculation presented before[14] can be also used for the comparison with MnO. In this paper we extend the theoretical results for Mn^{3+} in a spherically symmetric environment, and they are then compared with the experimental data for $LaMnO_3$.

II. EXPERIMENT

The experiment took place at beamline 8.0 at the Advanced Light Source of Lawrence Berkeley Laboratory. Monochromatized photons from a 5.0 cm undulator (U5.0) are focused onto the sample, and the resulting fluorescence emission spectra are recorded with a high efficiency x-ray spectrometer. This soft x-ray fluorescence spectrometer is a grazing incidence instrument with a fixed entrance slit and a position-sensitive area detector. A total electron yield (TEY) spectrum is obtained by recording the total electric current through the sample as the energy of the exciting photons is scanned. Photon emission spectra are then recorded at selected values of the incoming photon energy by positioning the spectrometer detector along the Rowland circle to intercept the wavelength region of interest. Details of the beam line and the spectrometer have been published elsewhere.[15] The incoming radiation flux was monitored by the total photocurrent produced in a gold mesh placed in front of the beam just before the sample chamber. The monochromator and the spectrometer energies were calibrated with the absorption and emission spectra of the metallic manganese sample. The absorption and emission experimental values in metallic manganese were fixed to those published in the literature.[16,17] We took a metallic manganese reference emission spectrum before recording the series of emission spectra for each sample. The metallic manganese sample was a commercially available chip of purity greater than 99.9%, though it was exposed to atmosphere before loading it into the experimental chamber and therefore its surface was oxidized. The MnO and MnF_2 samples were commercial powders of purity greater than 99%. The $LaMnO_3$ was a single crystal. For the MnF_2, MnO, and the metal emission spectra, we used an angle of incidence of 45° with respect to the incoming radiation, and therefore the fluorescence also made an angle of 45° with respect to the sample normal. In order to increase the count rate for $LaMnO_3$ we had to increase the angle of incidence to 55°, and we also increased the monochromator exit slit aperture. This should have little effect, however, on the relative intensities of the emission peaks.

III. RESULTS AND DISCUSSION

A comparison of the TEY spectra of MnF_2, metallic manganese, MnO, and $LaMnO_3$ is made in Fig. 1. The lower case labels in the MnF_2 spectrum indicate the values of the exciting photon energy at which we recorded the $3s \rightarrow 2p$ photon

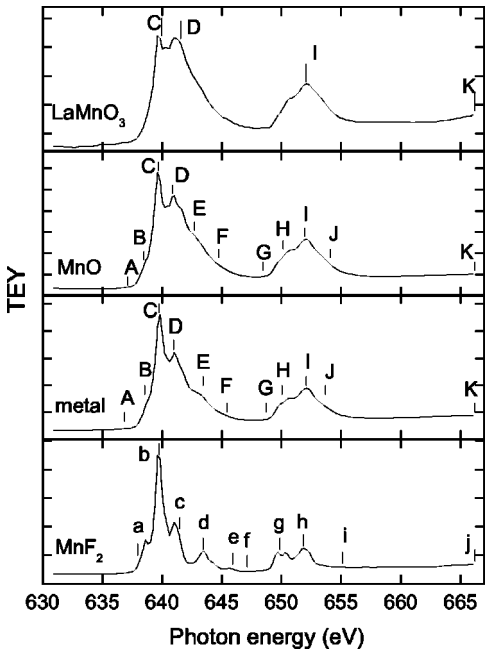

FIG. 1. Total electron yield (TEY) spectra of MnF_2, metallic manganese, MnO, and $LaMnO_3$ in the region of the $2p \rightarrow 3d$ resonances. The labels give the excitation energies at which we obtained $3s \rightarrow 2p$ emission spectra. The photon energy scale is the same in all spectra, while the vertical scale is arbitrary in each case.

emission spectra that are analyzed in detail elsewhere.[14] The upper case labels in the metallic manganese, MnO, and $LaMnO_3$ spectra also give the values of the photon energy for which we recorded emission spectra. The TEY spectrum of both metallic manganese and MnO were recorded directly from the samples, and therefore show indication of an oxide surface,[6] even for MnO. In Ref. 6 it was shown that the signal from the oxide layer can be removed by sputter cleaning the sample. If we compare our TEY spectra with those of Ref. 6 it is clear that our MnO TEY spectrum is almost identical to their spectrum for the oxidized sample, and their clean MnO spectrum is almost the same as our MnF_2 spectrum that has been shown to correspond to Mn^{2+} absorption.[14] They also showed[6] that a direct subtraction between the original spectrum of the oxidized sample and that of the clean sample resulted in a Mn^{3+} absorption signal. Here we follow a similar procedure to subtract the Mn^{2+} spectrum obtained in MnF_2 from each of our TEY spectra. The results are shown in Fig. 2. The bottom panel is, once more, the MnF_2 total electron yield. In the top panel we show the signal that has to be added to the bottom panel to obtain the spectra in Fig. 1. It is clear that in all cases the subtraction gives spectra that correspond to Mn^{3+}.[6] In fact, the result for MnO is in good agreement with Ref. 6. We notice that there are some differences among the subtracted spectra, mainly in the region of the L_3 edge. The signal for the metal does not show a defined structure, while the MnO and $LaMnO_3$ have a pre-edge peak and two distinctive peaks at 640.3 and 641.7 eV. However, the intensity ratio of these two peaks is different for each compound. They are both about equal for MnO, while in $LaMnO_3$ the second peak is larger. In $LaMnO_3$ there is also an indication of structure at

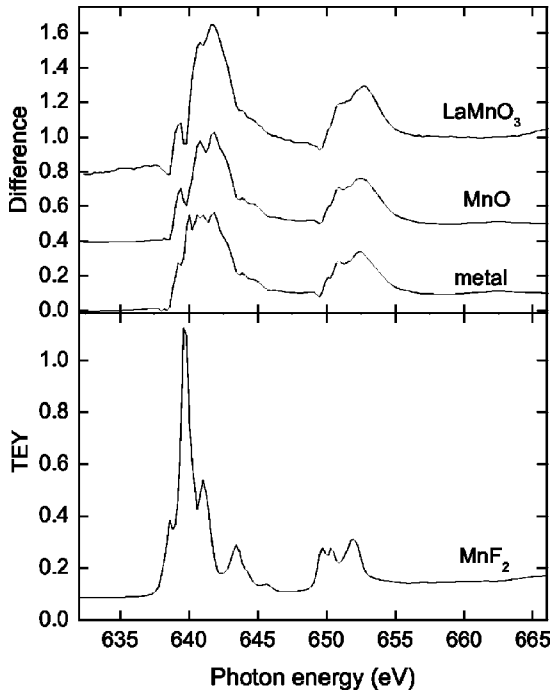

FIG. 2. Result of subtracting the MnF_2 TEY spectrum from the spectra of metallic manganese, MnO, and $LaMnO_3$.

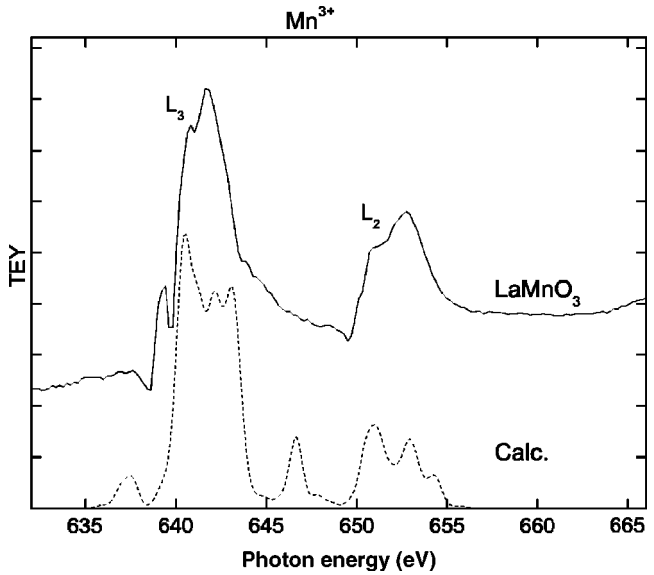

FIG. 3. Comparison between the Mn^{3+} TEY spectrum of $LaMnO_3$ and the result of a free-ion calculation. Solid line: experimental data. Dashed line: calculation. The L_3 and L_2 absorption edges are also indicated.

low photon energies, around 637 eV. The L_2 absorption features on the high-energy side are almost identical for all three samples. The fact that we were able to subtract a significant Mn^{2+} absorption signal in $LaMnO_3$ is in agreement with the results of a cluster calculation[20] that indicates that the ground state is an almost equal admixture of d^4 and $d^5\underline{L}$ states, where this last term denotes a state in which a ligand electron is transferred to the manganese ion.

In our previous work,[14] we showed that the TEY spectrum of MnF_2 can be interpreted directly in terms of Hartree-Fock (HF) calculation for the Mn^{2+} free ion. All the lines correspond to electric-dipole excitations starting in a $3d^5\ ^6S$ ground-state configuration. In this paper we make the corresponding comparison between the results of a calculation for a Mn^{3+} free ion and the subtracted signal for $LaMnO_3$. The calculation considers transitions starting at the $3d^4\ ^5D$ ground term, but in this case there are five possible values of the total angular momentum. We included all transitions originating in these states, weighted by their corresponding Boltzmann and degeneracy factors. We used the standard 80% contraction factors for the Slater integrals to partially take into account the effect of correlation.[18] The calculated spectrum is presented at the bottom of Fig. 3. The experimental Mn^{3+} spectrum for $LaMnO_3$ in Fig. 2 is shown on top. The theoretical spectrum was shifted down in energy to make the peaks at 640.7 eV coincide. In this case the free-ion calculation is not as successful as for Mn^{2+}.[14] It gives the right energy separation between the L_3 and L_2 absorption edges. It also predicts a small peak at 637 eV that would correspond to the pre-edge structure in the experimental spectrum. However, this structure is broader and asymmetric in the experimental spectrum. The calculation predicts three peaks at the L_3 and only two appear in the experimental data. The first peak in the calculation is the strongest, and in $LaMnO_3$ the second peak is the largest. The calculation predicts a peak at about 646 eV that is completely absent from the experimental spectrum. Finally, both experiment and theory give a three peak structure in the region of the L_2 edge, between 650 and 655 eV, but the calculation gives sharper peaks and in the reversed order of intensity.

In these experiments we also recorded the $3s \rightarrow 2p$ emission spectra at selected points in the TEY spectra, indicated by C, D, I, and K in Fig. 1. In MnO and $LaMnO_3$ the $3s \rightarrow 2p$ emission features are about 20 eV higher in energy with respect to the intense oxygen $2p \rightarrow 1s$ emission. They are, therefore, superimposed on top of a rather large background. This background also appears in the metallic manganese data, suggesting the presence of an oxide layer. In fact, for the metal, MnO, and $LaMnO_3$, we were able to obtain spectra containing both oxygen 1*s* and manganese 3*s* emission peaks, though there is definitely a larger oxygen background component in the MnO and $LaMnO_3$ samples.

We start the 3*s* emission comparison with the spectrum obtained 16 eV above the resonance structure (Fig. 4). This is much larger than the 2*p*-hole-width, and we therefore expect that in these spectra, emission is completely decoupled from absorption. In our previous analysis,[14] we made a detailed study of this "normal" emission for MnF_2 and also gave a theoretical interpretation based on a multiconfigurational HF calculation that includes the interaction of the 3*s* hole in the final state with the $3p^43d^6$ configuration. In Fig. 4 we make a comparison among the "normal" emission spectra of all samples. The dots are the experimental spectra, while the continuous lines give the result of a four peak fit to the data, with the background subtracted. We used Pearson-7 functions[19] with the same width and peak shape parameter for all peaks. This allowed us to continuously vary the peak shape between a Lorentzian and a Gaussian. The results ob-

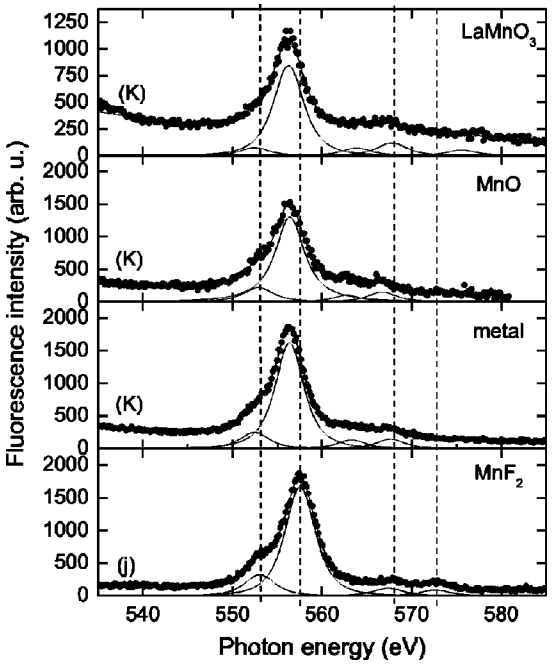

FIG. 4. Normal 3*s* emission spectrum for MnF_2, metallic manganese, MnO, and $LaMnO_3$. The excitation energy is indicated by (j, K, K, K) in Fig. 1. The dots are the experimental data. The continuous line gives the best fit through the dots, including an exponential background. The dashed lines are the individual peaks. The vertical lines give the position of the emission peaks in MnF_2.

tained in the fits indicate that in all cases the peak shape is predominantly Lorentzian. The measured line width is about 3.8 eV and it is almost the same for all samples. For comparison purposes we indicate with vertical lines the position of each of the peaks in MnF_2. All the compounds show the same overall structure with a strong peak, a low-energy shoulder, and two small peaks on the high-energy side. This structure can be explained by emission between a state in which the $2p$ hole couples to the $3d^5\ ^6S$ subshell, resulting in either a ^7P or ^5P term, and a state with a $3s$ hole.[14] The two emission peaks lower in energy are dominated by transitions into a $2p_{3/2}$ hole, while the two features at higher energies result from transitions into a $2p_{1/2}$ hole. This behavior, which is very well described by the calculation in MnF_2, is also present in all the other samples, even in the nominally Mn^{3+} compound $LaMnO_3$. At this point we remark that the relative position of the peaks is different for each sample. Compared to MnF_2, the whole emission structure is compressed and slightly shifted towards lower emission energies in the other compounds. In addition, there is an extra emission peak in $LaMnO_3$, at about 575 eV. Taking the difference between centers of the highest and the rest of the peaks as an indication of the spread, one measures an energy spread of 19.6 eV for MnF_2, 15.2 eV for the metal, 13.8 eV for MnF_2, and 15.3 eV for $LaMnO_3$. The main emission peak is pretty much in line for the metal, MnO, and $LaMnO_3$, and is clearly shifted down with respect to the main peak in MnF_2. The shoulder to the low-energy side is almost at the same energy in all compounds, the largest shift being 0.6 eV towards lower emission energy in the metal.

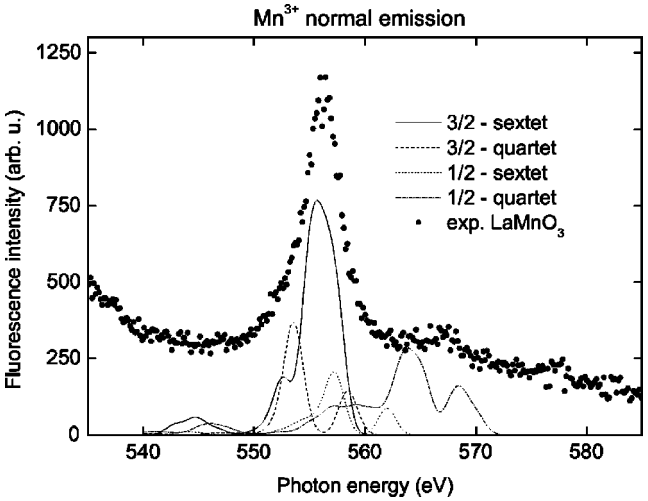

FIG. 5. Comparison between the $Mn^{3+}3s$ "normal" emission spectrum and the experimental data for $LaMnO_3$. Dots: experimental results. The theoretical results are indicated as follows. Solid line: emission from $2p_{3/2}3d^5(^5D)$ sextet states. Dashed line: emission from $2p_{3/2}3d^5(^5D)$ quartet states. Dotted line: emission from $2p_{1/2}3d^5(^5D)$ sextet states. Dash-dotted line: emission from $2p_{1/2}3d^5(^5D)$ quartet states.

There are also differences in the relative intensities of the emission peaks. The relative intensity of the low-energy shoulder at 553 eV is largest for MnF_2, then decreases slightly for MnO and the metal, and is a factor of 3 smaller for $LaMnO_3$. The relative intensities of the two emission peaks on the high-energy side also depend strongly on the compound. In MnF_2 the first peak is about 32% larger than the second and they are almost equal in the metal, and in MnO the second peak is 47% larger than the first. In $LaMnO_3$ the first peak of this group is 67% larger than the second. The extra peak in $LaMnO_3$ is the smallest of the group.

We also performed a HF calculation for "normal" emission from a nominal Mn^{3+} ion in the ground state. In this case we made the same assumption as before,[14] namely, that after direct production of a $2p$ hole it only couples to the high-spin terms $3d^4\ ^5D$. One then finds that a number of states are produced and they roughly correspond to high-spin sextet terms and low-spin quartet terms. Here we stress that this approximate term assignment by no means implies that these are pure states, because the Coulomb interaction and the $2p$ hole spin-orbit coupling strongly mix different states. In the end, however, a rather similar structure is found for the $3s$ decay, with four broad features. A comparison between the calculated emission and the $3s$ "normal" spectrum of $LaMnO_3$ is shown in Fig. 5. The comparison between experiment and theory is certainly not as good as the one found[14] for MnF_2. However, we find the same overall structure, a strong peak corresponding to decay from the $2p_{3/2}3d^5$ sextet terms, and a low-energy quartet shoulder. The calculation gives two peaks at higher energy, both resulting from the decay of a $2p_{1/2}$ hole. Experimentally, we observe the $2p_{3/2}$ and the $2p_{1/2}$ peaks at the calculated energies, and another broad and weak peak at a higher emission energy. The calculation also predicts a broad, low-energy satellite at about

TABLE I. High-spin to low-spin energy splittings (eV).

Compound	Photoemission	$2p_{3/2}$ fluorescence	$2p_{1/2}$ fluorescence
MnF_2	6.5[a]	4.5	5.2
Metal		3.9	4.3
MnO	6.2[b]	3.5	3.9
$LaMnO_3$	5.6[b]	3.8	3.9

[a]Also for atomic manganese (see, also, Ref. 22).
[b]Ref. 23.

545 eV, however, no indication of its existence is found in the experimental data. These results would seem to indicate that "normal" emission is dominated by the 3*s* hole and its interaction with the configuration with two 3*p* holes, and that the detailed structure of the outer 3*d* subshell plays a minor role.

From this analysis it is clear that the nondispersive or "normal" $3s \rightarrow 2p$ emission has a similar structure in all compounds studied. However, the position and relative intensity of each peak depend on the detailed electronic structure of the compound. The change in the peak position depends on the changes in the energy levels owing to the presence of the crystal field, while the relative peak intensity depends on the electric-dipole transition-matrix element that is also dependent on the detailed electronic structure. It is interesting to point out that the measured changes in separation between the low-energy and high-energy doublet that is due mainly to the 2*p* fine structure would seem to indicate that this splitting is affected by the valence-band structure. The largest measured splitting is 15.1 eV for MnF_2, and the smallest is 10.3 eV for MnO. Taking the differences between the two low-energy peaks and between the two high-energy peaks one can also obtain values for the high-spin to low-spin splitting in the 3*s* subshell. These values can be compared to the splittings obtained directly in photoemission,[22,23] but one has to keep in mind that our values are certainly reduced by the presence of the 2*p* hole. The comparison is made in Table I. The effect of the 2*p* hole is to reduce the splitting, and it is larger for the $2p_{3/2}$ hole. No systematic trend in the splitting is found as a function of the manganese valence state.

Finally, a word about the extra peak at 575 eV in $LaMnO_3$. This feature is definitely too high in energy, and would seem to correspond to the $3p \rightarrow 2p_{3/2}$ nondipole emission found in other transition-metal compounds.[24] It is 19 eV above the main 3*s* emission peak, while theory puts it at about 30 eV.[17] The fact that it appears only in $LaMnO_3$, a distorted perovskite, would seem to indicate that its intensity is enhanced by the lack of inversion symmetry at the metal site.

Now we compare the emission spectra obtained at corresponding points in the TEY spectra. We took emission spectra at resonances C, D, and I in Fig. 1, and thus we are able to compare the emission features for the metal, MnO, and $LaMnO_3$ at these resonances with the emission spectra for MnF_2 at resonances b, c, and h, analyzed separately.[14]

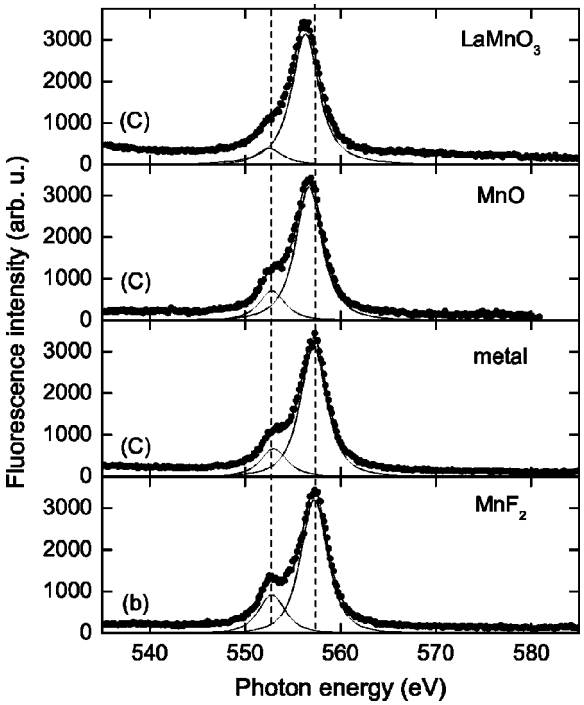

FIG. 6. Emission spectra at the maximum of the $Mn^{2+}L_3$ resonance (b, C, C, C) in Fig. 1. The symbols are the same as in Fig. 4.

The comparison of emission at the first resonance is made in Fig. 6. Once again, the dots represent the normalized data, while the continuous line represent the fitted peaks and the dashed line indicates the peak position obtained for MnF_2. These were the emission spectra used for normalization, in order to make the height of the most intense peak the same in all compounds for this particular excitation energy. In the calculation discussed in Ref. 14 we found that in the Mn^{2+} ion this resonance is dominated by a ^6P term that then decays into ^4D and ^6D terms. We observe a similar behavior for all compounds, indicating that at this photon energy both absorption and 3*s* emission are produced by Mn^{2+} ions in the sample. There are two peaks in each spectra, with comparable relative intensities, but there are measurable differences among the compounds. The ^4D shoulder at the low-energy side is at about the same position in all the spectra. The ^6D main peak is at about the same position in MnF_2 and the metal, and is shifted towards lower emission energies in MnO and $LaMnO_3$. The separation between the two peaks is reduced from the value in MnF_2, to the metal, until it becomes 3.8 eV in both MnO and $LaMnO_3$. This last value is closer to the one obtained in the ionic HF calculation.[14] There are also variations in the intensity of the ^4D peak relative to the ^6D peak. It is largest for MnF_2, about the same for the metal and MnO, and smallest for $LaMnO_3$. All of these values are smaller than the calculated free-ion relative intensity.[14]

Figure 7 shows the emission spectra at the second resonance of the $2p_{3/2}$ group (c in MnF_2 and *D* for the other compounds). In MnF_2 this corresponds to excitation into a ^4D state in Mn^{2+}. However, in the other compounds this resonance coincides with the strongest transition in Mn^{3+}. One would therefore expect that any difference of the 3*s*

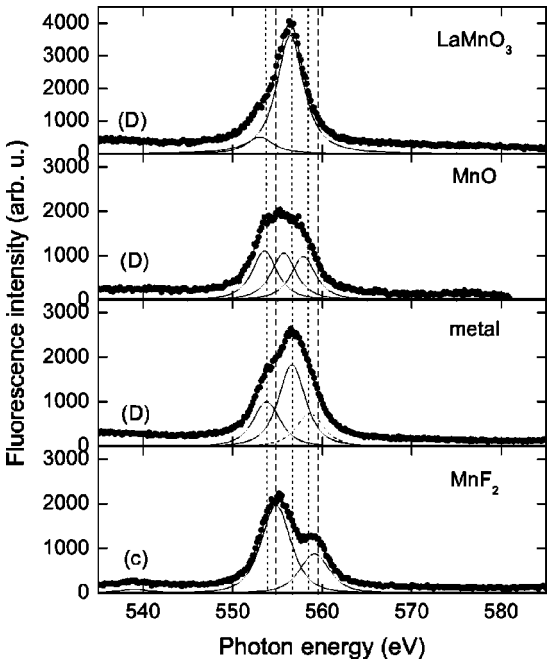

FIG. 7. Emission spectra at the maximum of the $Mn^{3+}L_3$ resonance (c, D, D, D) in Fig. 1. The symbols are the same as in Fig. 4.

emission compared to MnF_2 is caused by the presence of Mn^{3+} ions. In MnF_2 the 3*s* emission proceeds mainly into the ^4D and ^6D channels, producing two peaks. The largest contribution results from the state with the same dominant multiplicity as the intermediate state, which is a quartet. This agreement between theory and experiment indicates that for MnF_2 the interference effects that were neglected in the calculation play only a minor role in this compound. The situation is certainly different in the metal and in MnO. For these two samples there is a broad feature that can be adequately fitted by three peaks. The peaks at the highest and lowest emission energies seem to be aligned in these two compounds, and they are likely to correspond to emission into the $3s^4D$ and $3s^6D$ states found in MnF_2, provided they are shifted down. The peak at the center would then correspond to the main emission peak in $LaMnO_3$ and it can be readily identified with "normal" emission into a $2p_{3/2}$ hole produced nonresonantly. This competition between Raman and "normal" emission has been observed before[21] in CoO and NiO, and was interpreted as resulting from the creation of electron-hole pairs across the gap. However, in our results for $LaMnO_3$ this emission feature is really dominant and does not disappear when the excitation energy is more than a few eV above threshold.

Figure 8 shows the comparison between the experimental emission spectrum and the result of the calculation for "normal" emission, in which we present the features that correspond to decay of the $2p_{3/2}$ hole. The main peak in the calculation corresponds to the high-spin sextet states, and is shifted to lower energies with respect to the maximum in the experimental data, probably indicating the presence of a dispersive peak. The quartet shoulder is certainly visible in the experimental spectrum.

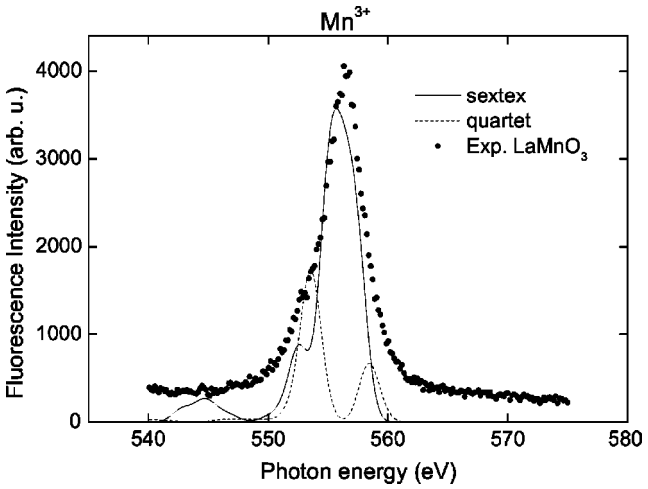

FIG. 8. Comparison between the $LaMnO_3$ emission spectrum at resonance D with the calculation for "normal" $2p_{3/2}$ emission. Dots: experimental data. The theoretical results are indicated as follows. Solid line: decay from the $2p_{3/2}3d^4\ ^5D$ sextet terms. Dashed line: decay from the $2p_{3/2}3d^4\ ^5D$ quartet terms.

This competition between resonant and "normal" $3s \rightarrow 2p$ emission is also displayed in the spectra shown in Fig. 9. Here we present the emission spectra that correspond to the excitation energies indicated by *h* in MnF_2 and I in all the other compounds. In this case we have two excitation mechanisms. We have a resonant transition that produces a $2p_{1/2}$ hole and we also have a nonresonant excitation in which a $2p_{3/2}$ hole is produced, with direct excitation of the electron into the conduction band. We also have to consider the Coster-Kronig process that transfers the $2p_{1/2}$ hole into

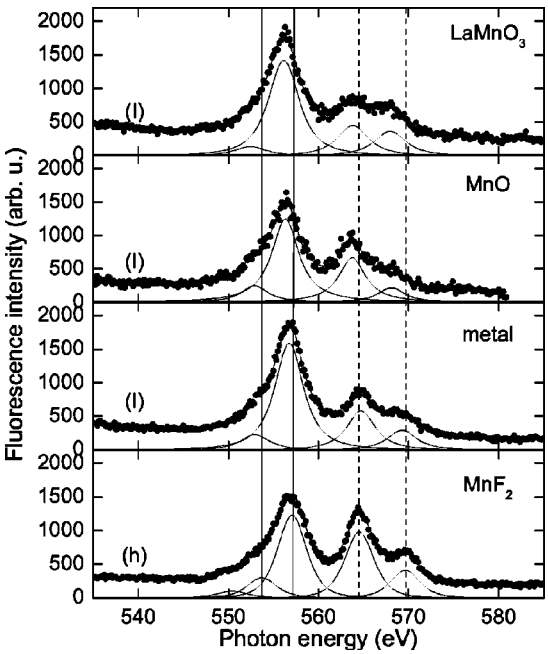

FIG. 9. Emission spectra at the maximum of the $3p^53d^6\ ^4D$ resonance (h, I, I, I) in Fig. 1. The position of the "normal" $3s \rightarrow 2p_{3/2}$ emission peaks is indicated by solid lines, while that of the resonant $3s \rightarrow 2p_{1/2}$ peaks is indicated by dashed lines.

the $2p_{3/2}$ hole. This process will enhance the "normal" emission to fill the $2p_{3/2}$ hole. In the last two cases, and considering the Mn^{2+} ionic model, this would lead to nonresonant x-ray emission starting in a $2p_{3/2}^5 3d^5$ configuration. The features that correspond to this "normal" emission are the two peaks on the low-energy side of each spectrum (indicated by solid lines), while the two peaks on the high-energy side are the resonant ones (indicated by dashed lines). Taking the peak with maximum intensity in MnF_2 as a reference for the emission energy, it is clear that the corresponding peak in the other compounds is shifted towards lower energies, with the largest shift occurring for MnO and $LaMnO_3$. The resonant structure is at about the same energy in the metal and in MnF_2, and is shifted towards lower energies in MnO and $LaMnO_3$. More importantly, the intensity of the resonant structure relative to the "normal" $3s \rightarrow 2p_{3/2}$ is certainly different for each compound. In MnF_2 this relative intensity is the largest and then it decreases for MnO and $LaMnO_3$, and is smallest for the metal.

IV. CONCLUDING REMARKS

In this article we presented results for manganese x-ray absorption and 3*s* emission for excitation energies across the *L* absorption edges and for different compounds. We find from the absorption spectra that the Mn^{2+} free-ion behavior is dominant for MnF_2. We also found that a signal produced by Mn^{3+} absorption is present in the spectra of metallic manganese and MnO, indicating the presence of a surface oxide layer or mixed valence in the metal. However, the 3*s* x-ray emission results indicate some degree of mixed valence states in these compounds. The absorption spectrum of $LaMnO_3$ is also a superposition of absorption by Mn^{2+} and Mn^{3+} ions. We found out that the free-ion calculation for Mn^{3+} is not as successful as the Mn^{2+} free-ion calculation for MnF_2, something that suggests a mixed valence for $LaMnO_3$. It is also clear that chemical effects are present in the manganese $3s \rightarrow 2p$ emission after resonant excitation of the $2p$ core electron in all compounds studied. There are systematic trends in this study that indicate that the pure ionic behavior found for MnF_2 is dominated by resonant emission. In the metal and the more hybridized compounds the normal emission that results when the excited electron interacts weakly with the 3*d* subshell is more important.

ACKNOWLEDGMENTS

We acknowledge support from DOE-EPSCOR cluster research Grant No. DOE-LEQSF (1993-1995)-03. The Advanced Light Source is funded by the Office of Basic Energy Science, U.S. Department of Energy Contract No. DE-AC03-76SF00098. JJM was supported in part by CONACyT, México, under Project No. U41007-F.

*Email address: jimenez@nuclecu.unam.mx

[1] S. P. Cramer, F. M. F. deGroot, Y. Ma, C. T. Chen, F. Sette, C. A. Kipke, D. M. Eichhorn, M. K. Chan, W. H. Armstrong, E. Libby, G. Christou, S. Brooker, V. McKee, O. C. Mullins, and J. C. Fuggle, J. Am. Chem. Soc. **113**, 7937 (1991).

[2] M. M. Grush, Y. Muramatsu, J. H. Underwood, E. M. Gullikson, D. L. Ederer, R. C. C. Perera, and T. A. Callcott, J. Electron Spectrosc. Relat. Phenom. **92**, 225 (1998).

[3] M. M. Grush, C. R. Horne, R. C. C. Perera, D. L. Ederer, S. P. Cramer, E. J. Cairns, and T. A. Callcott, Chem. Mater. **12**, 659 (2000).

[4] J. Kawai, Y. Mizutani, T. Sugimura, M. Sai, T. Higuchi, Y. Harada, Y. Ishiwata, A. Fukushima, M. Fujisawa, M. Watanabe, K. Maeda, S. Shin, and Y. Gohshi, Spectrochim. Acta, Part B **55**, 1385 (2000).

[5] C. R. Horne, U. Bergmann, M. M. Grush, R. C. C. Perera, D. L. Ederer, T. A. Callcott, E. J. Cairns, and S. P. Cramer, J. Phys. Chem. B **104**, 9587 (2000).

[6] B. Gilbert, B. H. Frazer, A. Belz, P. G. Conrad, K. H. Nealson, D. Haskel, J. C. Lang, G. Srajer, and G. De Stasio, J. Phys. Chem. A **107**, 2839 (2003).

[7] F. de Groot, Chem. Rev. (Washington, D.C.) **101**, 1779 (2001).

[8] P. S. Bagus, R. Broer, W. A. de Jong, W. C. Nieuwpoort, F. Parmigiani, and L. Sangaletti, Phys. Rev. Lett. **84**, 2259 (2000).

[9] S. M. Butorin, J.-H. Guo, M. Magnuson, P. Kuiper, and J. Nordgren, Phys. Rev. B **54**, 4405 (1996).

[10] D. L. Ederer, J. A. Carlisle, J. Jiménez, J. J. Jia, K. Osborn, T. A. Callcott, R. C. C. Perera, J. H. Underwood, L. J. Terminello, A. Asfaw, and F. J. Himpsel, J. Vac. Sci. Technol. A **14**, 859 (1996).

[11] J. Jiménez-Mier, U. Diebold, D. L. Ederer, T. A. Callcott, M. Grush, and R. C. Perera, Phys. Rev. B **65**, 184105 (2002).

[12] M. Taguchi, L. Braicovich, F. Borgatti, G. Ghiringhelli, A. Tagliaferri, N. B. Brookes, T. Uozumi, and A. Kotani, Phys. Rev. B **63**, 245114 (2001).

[13] L. Braicovich, M. Taguchi, F. Borgatti, G. Ghiringhelli, A. Tagliaferri, N. B. Brookes, T. Uozumi, and A. Kotani, Phys. Rev. B **63**, 245115 (2001).

[14] J. Jiménez-Mier, D. L. Ederer, and T. Schuler, Phys. Rev. A **68**, 042715 (2003).

[15] J. Jia, T. A. Callcott, J. Yurkas, A. W. Ellis, F. J. Himpsel, M. G. Samant, J. Stöhr, D. L. Ederer, J. A. Carlisle, E. A. Hudson, L. J. Terminello, D. K. Shuh, and R. C. C. Perera, Rev. Sci. Instrum. **66**, 1394 (1995).

[16] J. A. Bearden, Rev. Mod. Phys. **39**, 78 (1967).

[17] R. D. Deslattes, E. G. Kessler, Jr., P. Indelicato, L. de Billy, E. Lindroth, J. Anton, J. S. Coursey, D. J. Schwab, K. Olsen, and R. A. Dragoset, Rev. Mod. Phys. **75**, 35 (2003).

[18] R. D. Cowan, *The Theory of Atomic Structure and Spectra* (University of California Press, Berkeley, 1981).

[19] K. Pearson, Biometrika **16**, 157 (1924).

[20] T. Saitoh, A. E. Bocquet, T. Mizokawa, H. Namatame, A. Fujimori, M. Abbate, Y. Takeda, and M. Takano, Phys. Rev. B **51**, 13 942 (1995).

[21] F. Borgatti, L. Braicovich, N. B. Brookes, G. Ghiringhelli, and A. Tagliaferri, J. Electron Spectrosc. Relat. Phenom. **101**, 467 (1999).
[22] J. Jiménez-Mier, M. O. Krause, P. Gerard, B. Hermsmeier, and C. S. Fadley, Phys. Rev. A **40**, 3712 (1989).
[23] V. R. Galakhov, M. Demeter, S. Bartkowski, M. Neumann, N. A. Ovechkina, E. Z. Kurmaev, N. I. Lobachevskaya, Ya. M. Mukowskii, J. Mitchell, and D. L. Ederer, Phys. Rev. B **65**, 113102 (2002).
[24] J. Jiménez-Mier, D. L. Ederer, T. Schuler, and T. A. Callcott, J. Phys. B **36**, L173 (2003).